Journal of Environmental Management 147 (2015) 257–263

Contents lists available at ScienceDirect

Journal of Environmental Management

journal homepage: www.elsevier.com/locate/jenvman

# Oil removal from produced water by conjugation of flotation and photo-Fenton processes

Syllos Santos da Silva [a], Osvaldo Chiavone-Filho [a], Eduardo Lins de Barros Neto [a], Edson Luiz Foletto [b, *]

[a] Department of Chemical Engineering, Federal University of Rio Grande do Norte, Natal 59072-970, Brazil
[b] Department of Chemical Engineering, Federal University of Santa Maria, Santa Maria 97105-900, Brazil

ARTICLE INFO

*Article history:*
Received 5 November 2013
Received in revised form
5 June 2014
Accepted 27 August 2014
Available online 17 September 2014

*Keywords:*
Oilfield
Produced water
Flotation
Photo-Fenton
Integration

ABSTRACT

The present work investigates the conjugation of flotation and photo-Fenton techniques on oil removal performance from oilfield produced water. The experiments were conducted in a column flotation and annular lamp reactor for induced air flotation and photodegradation steps, respectively. A nonionic surfactant was used as a flotation agent. The flotation experimental data were analyzed in terms of a first-order kinetic rate model. Two experimental designs were employed to evaluate the oil removal efficiency: fractional experimental design and central composite rotational design (CCRD). Overall oil removal of 99% was reached in the optimum experimental condition after 10 min of flotation followed by 45 min of photo-Fenton. The results of the conjugation of induced air flotation and photo-Fenton processes allowed meeting the wastewater limits established by the legislations for disposal.



## 1. Introduction

Throughout the productive life of an oil field, the simultaneous production of gas, oil and water generally occurs. However, the economic interest is focused on the production of hydrocarbons (oil and gas), thus requiring the separation of these three fluids. The treatment of produced water (aqueous stream) aims to recover the dispersed oil and frame the final effluent for the purpose of reuse or disposal. In Brazil (CONAMA) and USA (USEPA), the maximum concentration of the total of oils and grease (TOG) in effluent disposal in the seabed is 29 ppm.

Several methods are applied to TOG reduction in aqueous effluents, such as liquid–liquid extraction (Moraes et al., 2011), hydrocyclones (Amini et al., 2012), flotation (Santo et al., 2012) and biological treatment (Lu et al., 2009). Among these methods, flotation is widely used because of its high rate of separation in short residence times and low operating cost (Watcharasing et al., 2008; Rattanapan et al., 2011; Le et al., 2013). This unit operation is based on differences in hydrophobicity among substances to be separated (Ding, 2010) and consists of the following steps (El-Kayar et al., 1993): (1) generation of bubbles, (2) contact between generated bubble and dispersed droplet, (3) formation of an aggregate bubble-droplet, (4) aggregate transportation.

The probability of flotation is defined as the product of the collision probabilities, adhesion and transport (Yoon, 2000). Eq. (1) shows that the probability of collision between the oil droplet and the air bubble is lower for small drops of oil.

$$P_C \alpha \left(\frac{D_g}{D_b}\right)^2 \quad (1)$$

where $D_g$ and $D_b$ are the diameters of the droplet and the bubble, respectively. This limitation is important in the treatment of produced water, where the oil could be present in four phases: free oil (droplets of oil >150 μm), dispersed oil (droplets of oil >50 μm), emulsified oil (droplets of oil <50 μm) and dissolved oil (Santander et al., 2011). Moreover, degradation of organic compounds present in effluents by Advanced Oxidation Processes (AOPs) has shown high efficiency even when they are present at low concentrations (Philippopoulos and Poulopoulos, 2003; Masomboon et al., 2010; Paz et al., 2013). Among AOPs, photo-Fenton is one of the most widely used techniques (Moraes et al., 2004a, 2004b; Nogueira et al., 2008; Sakkas et al., 2010; Nagarnaik and Boulanger, 2011). This process can be divided into three major steps (Krutzler and Bauer, 1999) (Eqs. (2)–(5)): (1) generation of hydroxyl radicals (•OH); (2) regeneration of ferrous ions by the action of light, (3)

* Corresponding author. Tel.: +55 55 3220 8448; fax: +55 55 3220 8030.
*E-mail address:* efoletto@gmail.com (E.L. Foletto).

http://dx.doi.org/10.1016/j.jenvman.2014.08.021
0301-4797/

oxidation of the organic matter by hydroxyl radicals present in the reaction medium.

$$Fe^{2+} + H_2O_2 \rightarrow Fe^{3+} + HO^{\bullet} \quad (2)$$

$$[Fe\ (OH)]^{2+} \xrightarrow{h\nu} Fe^{2+} + HO^{\bullet} \quad (3)$$

$$[Fe\ (COOCR)]^{2+} \xrightarrow{h\nu} Fe^{2+} + CO_2 + R^{\bullet} \quad (4)$$

$$HO^{\bullet} + RH \rightarrow \text{oxidation products} \rightarrow CO_2 + H_2O \quad (5)$$

Thus, a photodegradation step subsequent to the flotation process can improve oil removal efficiency in the effluent. Recently, some researchers have suggested the application of integrated processes as being the most appropriate solution for the treatment of various industrial effluents (Zak, 2009; Sena et al., 2009; Silva et al., 2012). Induced air flotation and photo-Fenton processes were integrated to the treatment of residual waters contaminated with xylene, resulting 100% of organic load removal in 20 min (Silva et al., 2012). Significant removal levels of chemical oxygen demand (COD) in treatment of oilfield wastewater containing polymers were obtained using the combination of the advanced oxidation by zerovalent iron/EDTA/air system followed by biodegradation process (Lu and Wei, 2011). Treatment of tannery industrial effluent by integrating the photo-Fenton and electrocoagulation processes resulted in an appreciable improvement in the results of COD removal when compared with the conventional process using a combination of filtration, chemical coagulation and sedimentation (Módenes et al., 2012). The integration of photocatalytic methods with a reverse osmosis unit can lead to complete decolorization of synthetic dye stuff effluent, as well as to a more than 95% reduction of the initial organic content (Berberidou et al., 2009). Oilfield wastewater treatment by combined microfiltration and biological processes may also result in a significant improvement in the effluent quality (Campos et al., 2002). Therefore, different combinations of processes can be applied for removing the several types of contaminants. Herein, the treatment of wastewater containing a real crude oil sample from Potiguar Basin (Natal, Brazil) was investigated with a conjugation of flotation and photochemical processes.

In this context, the aim of this study was to evaluate the integration of induced air flotation (IAF) and photo-Fenton processes for reducing the oil from oilfield produced water. From this integration, the aim was to recover the maximum amount of oil by flotation, and then degrade the remaining oil fraction in the aqueous phase by the photo-Fenton process.

## 2. Materials and experimental methodology

### 2.1. Crude oil

This study used a real crude oil sample from Potiguar Basin (Natal, Brazil). The oil was free of dissolved gas and water and its properties are summarized in Table 1.

### 2.2. Materials

A surfactant ethoxylated derived from fatty alcohol used as a flotation agent was supplied by Oxiteno®. Hydrophile-lipophile balance (HLB) and molecular mass of surfactant are 6.3 and 274 g $mol^{-1}$, respectively. The other used reagents were supplied by VETEC: sodium nitrate ($NaNO_3$), sodium chloride (NaCl), sodium sulfate ($Na_2SO_4$), potassium chloride (KCl), aluminum chloride ($AlCl_3$), magnesium chloride ($MgCl_2$) and calcium chloride ($CaCl_2$), ferrous sulfate heptahydrate ($FeSO_4.7H_2O$), hydrogen peroxide ($H_2O_2$, 30%) e chloroform ($CHCl_3$).

**Table 1**
Physical–chemical properties of crude oil.

| Physical–chemical property | Value |
|---|---|
| Density at 25 °C (g $mL^{-1}$) | 0.88 |
| API gravity (°API)[a] | 27 |
| Viscosity (cP) | 65.00 |
| Superficial tension (mN $m^{-1}$) | 29.95 |
| Interfacial tension (water/oil) (mN $m^{-1}$) | 10.98 |

[a] Calculated according to the relation $^{\circ}API = \left(\frac{141.5}{d_{60\,^{\circ}F}}\right) - 131,5$, where $d$ is the relative density.

Experiments were carried out using effluent prepared carefully from the dispersion of real crude oil in a saline aqueous solution containing: 17 ppm ($NaNO_3$), 4229 ppm (NaCl), 204 ppm ($Na_2SO_4$), 1497 ppm (KCl), 2.35 ppm ($AlCl_3$), 1506 ppm ($MgCl_2$) and 4875 ppm ($CaCl_2$). The selection and concentration of these salts was established from the average values found in the literature for oilfield produced water (USEPA, 2000; Campos et al., 2002; Ahmadun et al., 2009; Dong et al., 2011; Yeung et al., 2011; You and Wang, 2011). This effluent was stirred for 25 min at 33,000 rpm and then kept at rest for 50 min to allow free oil separation. Initial oil concentration in the effluent was 300 ppm and 35 ppm for the stages of flotation and photo-Fenton, respectively. These initial values of oil concentration were established on the basis of the average TOG of the effluents in the primary processing units of Potiguar basin, Brazil.

The determination of the TOG in aqueous samples was performed by liquid–liquid extraction, using chloroform as a solvent, followed by the measurement of the extract in molecular absorption spectrum, at $\lambda = 262$ nm (Varian, Cary 50) (Lima et al., 2008). The efficiency of each individual step ($\eta$) was expressed in terms of TOG removal (Eq. (6)), where $TOG_o$ and $TOG_t$ are the initial concentrations of oil and grease at $t = 0$ and time $t$, respectively. The measurements of oil/water interfacial tension were carried out by the drop method (tensiometer, 100 DAS).

$$\eta(\%) = \left(1 - \frac{TOG_t}{TOG_o} \times 100\right) \quad (6)$$

### 2.3. Experimental procedure of induced air flotation (IAF)

Flotation experiments were carried out in the flotation column using induced air aeration as a system for generating bubbles. Schematic diagram of column is shown in a previous work (Silva et al., 2012). Diffused air aeration was used, where the compressed air stream passed through a porous plate filter (16–40 μm) to form bubbles. The column with a capacity of 0.9 L has the following dimensions: 0.80 m (height), 0.040 m (inner diameter) and 0.042 m (external diameter). The initial pH (7.0) and the air flow (3.209 $cm^3$ m $in^{-1}$) values were kept constant for all the experiments. The addition of surfactant to the effluent was performed immediately before the beginning of the flotation step. At predetermined times (practically at each 2 min), samples were collected from the center of the column in order to determine the TOG value.

### 2.4. Photo-Fenton experimental procedure

The experiments were carried out in an annular reactor with a capacity of 0.6 L. A mercury vapor lamp was used as source of radiation (high pressure 400 W, FLZ) and located on the longitudinal

axis of the reactor, inside a quartz jacketed well with refrigerated water circulation. A schematic diagram of reactor is shown in a previous study (Silva et al., 2012). It is also noteworthy that the use of borosilicate glass or quartz for the reactor well will not affect the results of degradation using photo-Fenton process (Moraes et al., 2004a). The reactor is provided with an outer jacket to prevent overheating and to stabilize the temperature of the reaction medium. The system temperature was kept constant at 20 °C. The dosing of hydrogen peroxide was carried out continuously using a peristaltic pump. The effluent pH was adjusted to 3.0 with $H_2SO_4$. Iron sulfate ($FeSO_4.7H_2O$) and hydrogen peroxide ($H_2O_2$, 30%) were used as Fenton's reagents. The reaction mixture was provided by a magnetic stirrer. Samples were retrieved with the aid of a syringe in the bulk of the reaction medium. Practically one sample was withdrawn at each 5 min in order to determine the TOG concentration.

A full factorial design was conducted to evaluate the influence of the concentration of Fenton's reagents in reducing TOG. To carry out an experimental design with two independent variables ($n = 2$), seven experiments are needed in total, with four factorial points and three repetitions at the central point. Table 2 shows the coded levels of the studied variables. The experiments were carried out in order to obtain conditions for the maximum efficiency of mineralization. The order of the experiments was randomized to avoid any interference in the results.

## 3. Results and discussion

### 3.1. Reduction of TOG by flotation

Fig. 1 shows the curves of flotation efficiency for separation of the oil-water (O/W) system, where it can be seen that the presence of the surfactant contributes to the increase in the oil removal rate. For all concentrations tested, a high rate of separation was found in the first 4 min followed by a stabilization trend. The observed data were correlated with a first order kinetic model (Eq. (7)). Fig. 2 shows the linearization for oil removal for all concentrations of the surfactant employed. The fit quality was measured through determination coefficient ($R^2$). High values of the determination coefficient ($R^2 > 0.96$) demonstrated that the first order model was satisfactory to represent the reduction of TOG by flotation. This is in accordance with other research studies on the application of flotation to O/W systems (Kelebek and Nanthakumar, 2007; Uçurum, 2009; Silva et al., 2012).

$$\ln\left(\frac{C_0}{C}\right) = kt \tag{7}$$

where $C_0$ and $C$ are the initial oil concentrations ($t = 0$) and at time $t$ (mg $L^{-1}$), respectively; $k$ is the kinetic constant ($min^{-1}$) and $t$ is the flotation time (min).

First order kinetic considers that the bubble-particle collision rate is first order with respect to the number of particles and that bubble concentration remains constant over time (Eq. (7)) (Polat and Chander, 2000). Kinetic separation can also be correlated with the interfacial tension O/W (Fig. 3). It is possible to observe that the addition of a small amount of surfactant contributes to a

**Table 2**
Experimental design applied to TOG removal by photo-Fenton.

| Variable | $x_i$ | −1 | 0 | +1 |
|---|---|---|---|---|
| [Fe(II)] mM | $x_1$ | 0.10 | 0.27 | 0.44 |
| [$H_2O_2$] mM | $x_2$ | 10 | 27 | 44 |

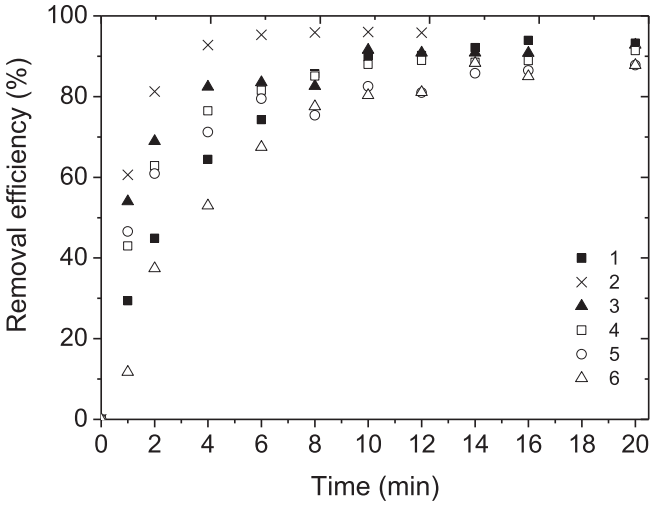


**Fig. 1.** Efficiency of oil removal by IAF using different surfactant concentrations: curve 1: absence of surfactant; curve 2: $4.06 \cdot 10^{-3}$ mM; curve 3: $9.43 \cdot 10^{-3}$ mM; curve 4: $2.86 \cdot 10^{-2}$ mM; curve 5: $6.82 \cdot 10^{-2}$ mM; curve 6: $1.21 \cdot 10^{-1}$ mM.

significant increase in the kinetic constant. However, an excess of surfactant may provoke a reduction in the separation rate. The interfacial tension (O/W) decreases as the surfactant concentration increases to a constant value. The surfactant tends to position itself at the interface, thereby reducing interfacial tension. For flotation of hydrophobic substances, which is the case of oils, this phenomenon is not desirable because it stabilizes the interface of the droplets, thus hindering coalescence. In the case of a surfactant with low hydrophilic characteristic, i.e., low BHL value (Griffin, 1949), such migration occurs into the oil droplet, due to high solubility in the oil phase, which promotes the breakdown of the oil droplet/air interfacial film before saturating the interface. Thus, flotation is favored when the surfactant is present at a low concentration. However, when an excess of this surfactant is used, the monomers migrate to the interface, saturating the oil droplet and, thus, becoming hydrophilic. The probability of adherence includes the time, thickness and rupture of the liquid film during the contact time. Oliveira et al. (1999) found that the induction time required

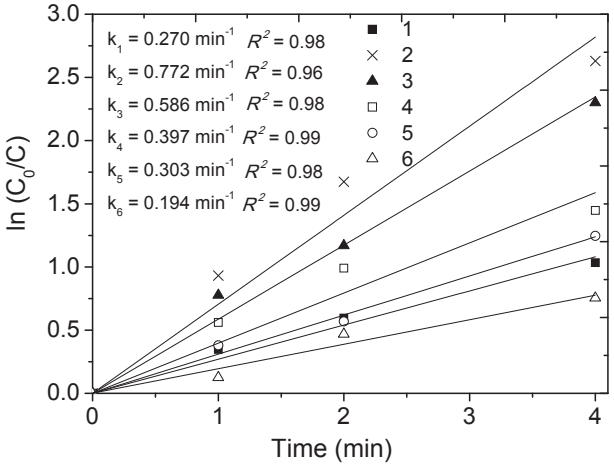


**Fig. 2.** Kinetic curves of oil removal by IAF using different surfactant concentrations at 4 min of flotation: curve 1: absence of surfactant; curve 2: $4.06 \cdot 10^{-3}$ mM; curve 3: $9.43 \cdot 10^{-3}$ mM; curve 4: $2.86 \cdot 10^{-2}$ mM; curve 5: $6.82 \cdot 10^{-2}$ mM; curve 6: $1.21 \cdot 10^{-1}$ mM. (Inset: kinetic constant values).

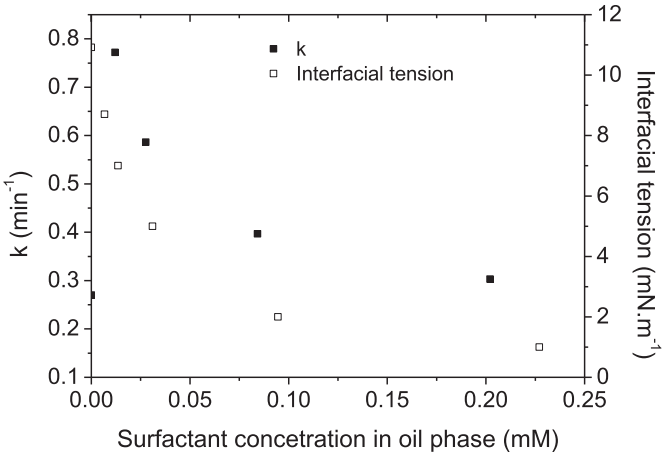


**Fig. 3.** Kinetic constant and interfacial tension (O/W) as a function of surfactant concentration at 4 min of flotation.

for bubble-droplet adhesion and spreading of the oil droplet in the bubble surface is determined by the affinity of the surfactant in relation to the phase in which it is dissolved. The results demonstrated that the increase of the surfactant concentration causes a reduction of induction time and an increase of the stabilization time. These researchers attributed this fact to the increase in the transfer of surfactant molecules across the interface, causing the rupture of the film to the contact point. This favors the adhesion and spreading of the oil droplet on the bubble.

### 3.2. Reduction of TOG by photo-Fenton

Previous work has demonstrated that gasoline degradation under conditions of photolysis (light UV only) was under than 6% (Moraes et al., 2004a). In addition, Fenton reaction ($H_2O_2/Fe^{2+}$), in the absence of UV irradiation, resulted in gasoline removal of approximately 20%. It is known that crude oil is more resistant than gasoline and thereby lower degradation values for these processes are expected. Therefore, a higher TOG removal for crude oil may be achieved with photo-Fenton reaction ($UV/H_2O_2/Fe^{2+}$).

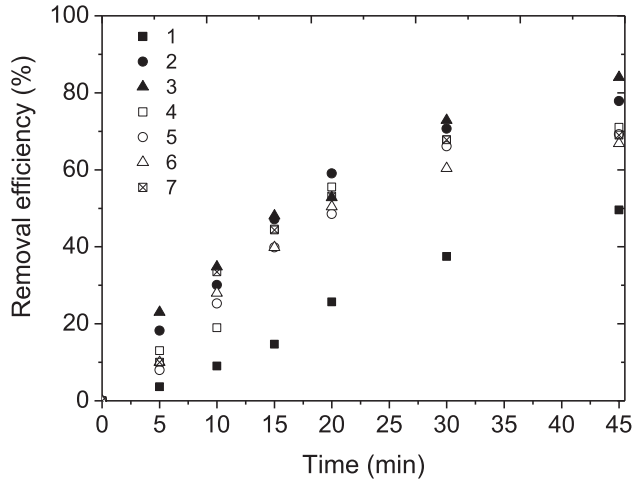


**Fig. 4.** The kinetic of TOG reduction by photo-Fenton according to the experimental design carried out: curve 1: 0.10 mM [Fe(II)] and 44 mM [$H_2O_2$]; curve 2: 0.10 mM [Fe(II)] and 10 mM [$H_2O_2$]; curve 3: 0.44 mM [Fe(II)] and 10 mM [$H_2O_2$]; curve 4: 0.44 mM [Fe(II)] and 44 mM [$H_2O_2$]; curves 5, 6 and 7: 0.27 mM [Fe(II)] and 27 mM [$H_2O_2$].

**Table 3**
Observed and predicted oil removal as a function of Fenton reagent (coded value) at 45 min.

| Run | $x_1$ | $x_2$ | Observed removal (%) | Predicted removal (%) |
|---|---|---|---|---|
| 01 | −1 | +1 | 50 | 49 |
| 02 | −1 | −1 | 78 | 77 |
| 03 | +1 | −1 | 84 | 83 |
| 04 | +1 | +1 | 71 | 70 |
| 05 | 0 | 0 | 69 | 70 |
| 06 | 0 | 0 | 67 | 70 |
| 07 | 0 | 0 | 69 | 70 |

The degradation kinetics of the photo-Fenton step was expressed in terms TOG removal (Eq. (6)). Fig. 4 shows kinetic curves of TOG removal by photo-Fenton following the conditions established in the experimental design (Table 2). Curve 3 (0.44 mM Fe(II) and 10 mM $H_2O_2$) showed the best efficiency with 84% of TOG reduction at 45 min of reaction, while curve 1 (0.10 mM Fe(II) and 44 mM $H_2O_2$) showed a lower efficiency.

The mathematical model that describes the response function ($y$) as a function of the dependent variables ($x_i$) is described by Eq. (8), where $y_i$ is the answer in the condition $i$, $x_i$ are the encoded levels for the independent variables, $\beta_0$, $\beta_i$, and $\beta_{ij}$ are the parameters of the regression model and $\varepsilon$ is the random error associated at this measure (Trinh and Kang, 2011). In this case, the estimated coefficients by the polynomial model were performed by the least squares method.

$$y_i = \beta_0 + \sum_{i=1}^{n} \beta_i x_i + \sum_{i<j}^{n} \beta_{ij} x_i x_j + \varepsilon \quad (8)$$

The response function ($y$) is expressed in terms of TOG reduction efficiency. The coefficients of the response function for the dependent variables were determined by correlating the experimental data with the response function using the software Statistica 7.0 (Eq. (9)).

$$y = 69.71 + 6.80x_1 - 10.21x_2 + 3.7x_1x_2 \quad (9)$$

Table 3 shows a comparison between the observed and the predicted values of oil degradation after 45 min of reaction. From the Pareto graph (Fig. 5), it is observed that all variables ($x_1$, $x_2$ and $x_1x_2$) of the model are statistically significant. The positive sign of the variable $x_1$ in the Pareto graph (Fig. 5) means that the increase

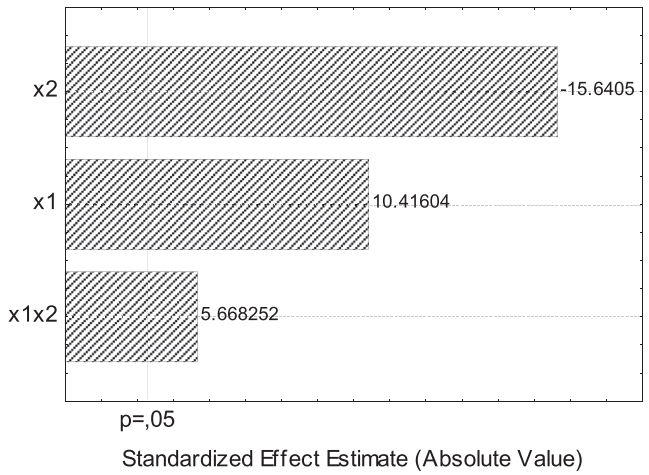


**Fig. 5.** Pareto graph for TOG removal by photo-Fenton as a function of ferrous ions ($x_1$) and hydrogen peroxide ($x_2$) concentrations.

**Table 4**
Analysis of variance (ANOVA) of TOG removal by photo-Fenton at 45 min.

| Source | Sum of squares | Degrees of freedom | Mean square | *F*-value | $F_{calculated}$ |
|---|---|---|---|---|---|
| Model | 657.41 | 3 | 219.14 | 51.15 | 9.28 |
| Residual | 12.85 | 3 | 4.28 | – | – |
| Lack of fit | 9.44 | 1 | 9.44 | 5.53 | 18.51 |
| Pure error | 3.41 | 2 | 1.71 | – | – |
| Total | 670.26 | 6 | | | |
| $R^2 = 0.9808$ | | | | | |
| $R^2_{adj} = 0.9616$ | | | | | |

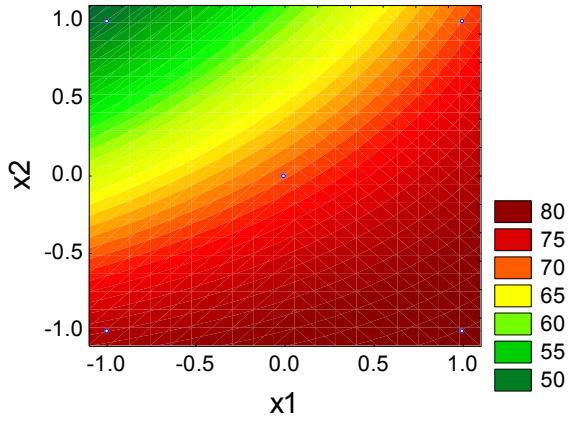


**Fig. 6.** Response surface of TOG removal efficiency by photo-Fenton as a function of ferrous ions ($x_1$) and hydrogen peroxide ($x_2$) concentrations.

in iron concentration favors oil degradation. This is due to greater availability of ferrous ions in the reaction medium to react with hydrogen peroxide and, thus, form hydroxyl radicals. Hydrogen peroxide concentration presented negative coefficient in the Pareto graph (Fig. 5) and, therefore, the increase of this variable disfavors oil removal. This effect may be attributed to the excess of hydrogen peroxide which leads to attack of the hydroxyl radical to hydrogen peroxide itself, resulting in the radical hydroperoxyl ($E^{\circ} = 1.8$ V) that has lower oxidation potential than the hydroxyl radical ($E^{\circ} = 2.8$ V) (Eq. (10)) (Dionysiou et al., 2000; Chu and Wong, 2004).

$$H_2O_2 + HO^{\cdot} \rightarrow HO_2^{\cdot} \quad (10)$$

Table 4 shows the Analysis of Variance (ANOVA) of the experimental results. From Fisher's distribution test, it was possible to verify that the proposed model is significant and predictive. The contour surface (Fig. 6) describes the experimental domain assessed and allows identifying the combination of levels of the variables $x_1$ and $x_2$ which leads to a greater efficiency. It can be seen that the variation of the ferrous ions concentration ($x_1$) of −1 level to +1 favors TOG reduction efficiency for both levels of variable $x_2$. On the other hand, the same variation in hydrogen peroxide concentration ($x_2$) leads to a reduction of up to 24% in removal efficiency. The synergetic effect among the variables, shown as significant in Pareto graph (Fig. 5), is evidenced in the contour surface (Fig. 6). From the contour surface, it can also be observed that the effect obtained by varying the level −1 to +1 of a variable, is dependent on the level of the other variable.

### 3.3. Reduction of TOG by integration of flotation and photo-Fenton

The integration process resulted in greater TOG reduction efficiency for each individual stage. In the flotation stage, the surfactant concentration was equal to $4.06 \cdot 10^{-3}$ mM, and for the photodegradation step, 0.44 mM Fe(II) and 10 mM $H_2O_2$ were used. The effluent was initially subjected to flotation and the treated liquid was collected from the bottom of the column and fed to the photochemical reactor. The flotation time ranged between 2 and 10 min and photodegradation was kept at 45 min for all experimental conditions (Table 5). The overall process efficiency was calculated according to Eq. (11), where $TOG_{a,PF}$ is the TOG value after the photo-Fenton step. The integration process time was determined by Eq. (12), where $t_F$ and $t_{PF}$ are the times of flotation and photo-Fenton steps, respectively.

$$\eta_{global}(\%) = \left(1 - \frac{TOG_0 - TOG_{a,PF}}{TOG_0}\right) \cdot 100 \quad (11)$$

$$t_{integrated\ process} = t_F + t_{PF} \quad (12)$$

Table 5 shows that the longer the flotation, the greater is the efficiency of the combined processes. For 10 min of flotation time, the overall integrated process efficiency was 99%, which represents a final disposal corresponding to 5 ppm of TOG. For 2 min of flotation time, the efficiency of this step was 74%, which implies a high concentration of oil which remains in the pretreated effluent (19 ppm), leading to a slower kinetics of the photochemical step. For the other conditions, such as 4 and 6 min, the overall efficiency was 95%, corresponding to 15 and 14 ppm of TOG, respectively. Although the difference between the overall efficiencies of the conditions corresponding to runs 1 and 4 was small in percentage terms, the flotation step is useful to recover the dispersed oil that can be sent for refining without loss of value and lower operating costs. Increasing the flotation time from 2 to 10 min represents an increase of 48 ppm in oil recovery (Table 5). Considering the huge amount of produced water generated in an oil production field, this amount of recovered oil can bring economic and environmental gains. On the other hand, the photochemical step is a chemical conversion step which converts oil to products such as $CO_2$ and $H_2O$, i.e., decomposing the oil and allowing the reuse of the treated water. Furthermore, flotation is limited by the diameter of the droplets, or flotation is hampered for very small droplets (dissolved oil fraction). Thus, the use of the photochemical step is justified in the integrated process because it removes the remainder TOG of the flotation stage. In this context, the photochemical step is proposed as a polishing step in the treatment of produced water. With the use of photo-Fenton, it was possible to reduce TOG to the level

**Table 5**
Efficiency of flotation and photo-Fenton combined to TOG removal ($TOG_0 = 300$ ppm).

| Run | Flotation time (min) | Flotation efficiency (%) | TOG after flotation (ppm) | Photo-Fenton time (min) | Photo-Fenton efficiency (%) | Process time (min) | Final TOG (ppm) | Integrated process efficiency (%) |
|---|---|---|---|---|---|---|---|---|
| 1 | 2 | 74 | 78 | 45 | 76 | 47 | 19 | 94 |
| 2 | 4 | 84 | 49 | 45 | 69 | 49 | 15 | 95 |
| 3 | 6 | 86 | 39 | 45 | 62 | 51 | 14 | 95 |
| 4 | 10 | 90 | 30 | 45 | 85 | 55 | 5 | 99 |

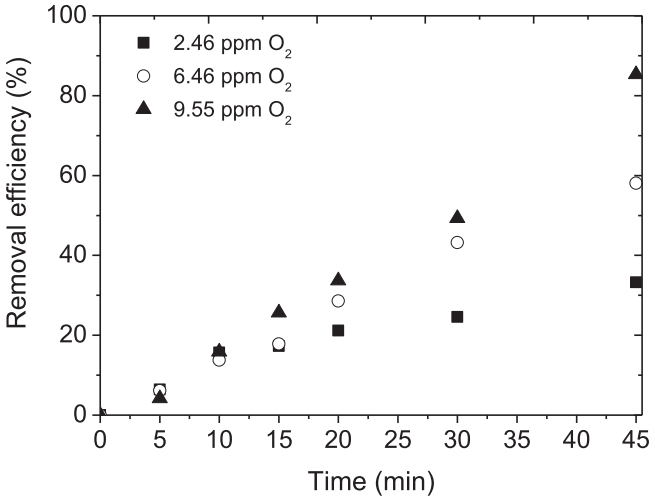


**Fig. 7.** Effect of dissolved oxygen ($O_2$) concentration in effluent on TOG removal by the photo-Fenton step.

established by the Brazilian (CONAMA) and American (USEPA) environmental legislations.

Photodegradation experiments were carried out to verify the influence of the concentration of dissolved oxygen and the results are reported in Fig. 7. In all cases, the initial TOG was kept constant at 30 ppm, iron concentration at 0.44 mM and hydrogen peroxide concentration at 10 mM. Dissolved oxygen concentrations were 2.46, 6.46 and 9.55 ppm and refer to the average values determined in the produced water, in the synthetic effluent (Millero et al., 2002) and after the flotation stage, respectively.

In Fig. 7, it can be observed that the increase of dissolved oxygen concentration promotes the photochemical step in the TOG reduction. Some researches (Sun and Pignatello, 1993; Kim et al., 1997; Utset et al., 2000; Du et al., 2007) indicated that the oxygen plays a positive role in the degradation of organic contaminants in Fenton and photo-Fenton processes. Thus, the integrated process that previously applies induced air flotation (IAF) contributes with the posterior step of photodegradation. This is also another synergetic effect of the proposed process for removing TOG in the produced water. Depending on the structure of the organic contaminant, the reactions with hydroxyl radicals can be triggered by different pathways: (i) abstraction of hydrogen atom, (ii) electrophilic addition to compounds containing unsaturated bonds and aromatic rings, and (iii) electron transfer and radical–radical reactions (Legrini et al., 1993). The reaction by hydrogen abstraction usually occurs with aliphatic hydrocarbons, where hydroxyl radicals oxidize organic compounds by hydrogen abstraction, generating organic radicals (Eq. (5)). Subsequently, addition of molecular oxygen produce peroxyl radicals (Eq. (13)), which initiate thermal reactions of degradation resulting into carbon dioxide, water and inorganic salts (Legrini et al., 1993).

$$R^{\cdot} + O_2 \rightarrow RO_2^{\cdot} \quad (13)$$

## 4. Conclusions

The experimental results of oil removal by flotation were described by a first-order kinetic model. For the evaluated surfactant concentrations, the highest removal rate ($k = 0.772\ min^{-1}$) was obtained at $4.06.10^{-3}$ mM and represents 86% of TOG reduction after 4 min of flotation. With respect to the photo-Fenton step, the highest oil removal achieved was 84% after 45 min of reaction, using 0.44 mM and 10 mM of ferrous ions and hydrogen peroxide, respectively. The best experimental condition found for the integrated processes was 10 min of flotation followed by 45 min of photo-Fenton with overall TOG reduction of 99%, which resulted in only 5 ppm of TOG in the treated effluent. The integration of the flotation and photo-Fenton processes proved to be very effective in reducing TOG in oilfield produced water. The following aspects have been evidenced in the integrated process studied: wastewater nature, i.e., dispersed and dissolved oil in the produced water; the addition of the surfactant agent at a limited concentration, and the use of air in the flotation stage, which promotes the photochemical degradation as a polishing role.

## Acknowledgments

Brazilian financial support provided by ANP (Agência Nacional do Petróleo, Gás Natural e Biocombustíveis), Petrobrás S.A, CAPES (Coordenação de Aperfeiçoamento de Pessoal de Nível Superior), CNPq (Conselho Nacional de Desenvolvimento Científico e Tecnológico) and INCT (Institutos Nacionais de Ciência e Tecnologia de Estudos Do Meio Ambiente) is gratefully acknowledged.

## References

Ahmadun, F.R., Pendashteh, A., Abdullah, L.C., Biak, D.R.A., Madaeni, S.S., Abidin, Z.Z., 2009. Review of technologies for oil and gas produced water treatment. J. Hazard. Mater. 170, 530–551.
Amini, S., Mowla, D., Golkar, M., Esmaeilzadeh, F., 2012. Mathematical modelling of a hydrocyclone for the down-hole oil–water separation (DOWS). Chem. Eng. Res. Des. 90, 2186–2195.
Berberidou, C., Avlonitis, S., Poulios, I., 2009. Dyestuff effluent treatment by integrated sequential photocatalytic oxidation and membrane filtration. Desalination 249, 1099–1106.
Campos, J.C., Borges, R.M.H., Oliveira-Filho, A.M., Nobrega, R., Sant'anna Jr., G.L., 2002. Oilfield wastewater treatment by combined microfiltration and biological processes. Water Res. 36, 95–104.
Chu, W., Wong, C.C., 2004. The photocatalytic degradation of dicamba in $TiO_2$ suspensions with the help of hydrogen peroxide by different near UV irradiations. Water Res 38, 1037–1043.
CONAMA – Conselho Nacional do Meio Ambiente – Resolução n° 393, de 8 de agosto de 2007. http://www.mma.gov.br/port/conama.
Ding, L.P., 2010. Effect of collector interfacial tension on coal flotation of different particle sizes. Ind. Eng. Chem. Res 49, 3769–3775.
Dionysiou, D.D., Suidan, M.T., Bekou, E., Baudin, I., Lainé, J.M., 2000. Effect of ionic strength and hydrogen peroxide on the photocatalytic degradation of 4-chlorobenzoic acid in water. Appl. Catal. B: Environ. 26, 153–171.
Dong, Z., Lu, M., Huang, W., Xu, X., 2011. Treatment of oilfield wastewater in moving bed biofilm reactors using a novel suspended ceramic biocarrier. J. Hazard. Mater. 196, 123–130.
Du, Y., Zhou, M., Lei, L., 2007. The role of oxygen in the degradation of *p*-chlorophenol by Fenton system. J. Hazard. Mater. 139, 108–115.
El-Kayar, A., Hussein, M., Zatout, A., Hosny, A., Amer, A., 1993. Removal of oil from stable oil-water emulsion by induced air flotation technique. Sep. Technol. 3, 25–31.
Griffin, W.C., 1949. Classification of surface active agents by HLB. J. Soc. Cosmet. Chem. 1, 311–326.
Kelebek, S., Nanthakumar, B., 2007. Characterization of stockpile oxidation of pentlandite and pyrrhotite through kinetic analysis of their flotation. Int. J. Min. Process 84, 69–80.
Kim, S.-M., Geissen, S.-U., Vogelpohl, A., 1997. Landfill leachate treatment by a photoassisted Fotin reaction. Water Sci. Technol. 35, 239–248.
Krutzler, T., Bauer, R., 1999. Optimization of a photo-Fenton prototype reactor. Chemosphere 38, 2517–2532.
Le, T.V., Imain, T., Higuchi, T., Yamamoto, K., Sekine, M., Doi, R., Vo, H.T., Wei, J., 2013. Performance of tiny microbubbles enhanced with normal cyclone bubbles in separation of fine oil-in-water emulsions. Chem. Eng. Sci. 94, 1–6.
Legrini, O., Oliveros, E., Braun, A.M., 1993. Photochemical processes for water treatment. Chem. Rev. 93, 671–698.
Lima, L.M.O., Silva, J.H., Patricio, A.A.R., Barros-Neto, E.L., Dantas-Neto, A.A., Dantas, T.N.C., Moura, M.C.P.A., 2008. Oily wastewater treatment through a separation process using bubbles without froth formation. Petrol. Sci. Technol. 26, 994–1004.
Lu, M., Wei, X., 2011. Treatment of oilfield wastewater containing polymer by the batch activated sludge reactor combined with a zerovalent iron/EDTA/air system. Bioresour. Technol. 102, 2555–2562.

Lu, M., Zhang, Z., Yu, W., Zhu, W., 2009. Biological treatment of oilfield-produced water: a field pilot study. Int. Biodeter. Biodeg. 63, 316–321.
Masomboon, N., Chen, C.-W., Anotai, J., Lu, M.-C., 2010. A statistical experimental design to determine o-toluidine degradation by the photo-Fenton process. Chem. Eng. J. 159, 116–122.
Millero, F.J., Huang, F., Laferiere, A.L., 2002. Solubility of oxygen in the major sea salts as a function of concentration and temperature. Mar. Chem. 78, 217–230.
Módenes, A.N., Espinoza-Quiñones, F.R., Borba, F.H., Manenti, D.R., 2012. Performance evaluation of an integrated photo-Fenton–Electrocoagulation process applied to pollutant removal from tannery effluent in batch system. Chem. Eng. J. 197, 1–9.
Moraes, J.E.F., Silva, D.N., Nascimento, C.A.O., Quina, F.H., Chiavone-Filho, O., 2004a. Treatment of saline wastewater contaminated with hydrocarbons by the Photo-Fenton process. Environm. Sci. Technol. 38, 1183–1187.
Moraes, J.E.F., Silva, D.N., Quina, F.H., Chiavone-Filho, O., Nascimento, C.A.O., 2004b. Utilization of solar energy in the photodegradation of gasoline in water and of oil-field-produced water. Environm. Sci. Technol. 38, 3746–3751.
Moraes, N.A., Paulo, J.B.A., Medeiros, G.S., 2011. Influence of main process variables on the treatment of wastewaters using a new technology (MSPI). Braz. J. Petrol. Gas 5, 75–85.
Nagarnaik, P.M., Boulanger, B., 2011. Advanced oxidation of alkylphenol ethoxylates in aqueouss systems. Chemosphere 85, 854–860.
Nogueira, K.R.B., Teixeira, A.C.S.C., Nascimento, C.A.O., Guardani, R., 2008. Use of solar energy in the treatment of water contaminated with phenol by photochemical processes. Braz. J. Chem. Eng. 25, 671–682.
Oliveira, R.C.G., Gonzalez, G., Oliveira, J.F., 1999. Interfacial studies on dissolved gas flotation of oil droplets for water purification. Coll. Surf. A: Physicoch. Eng. Asp. 154, 127–135.
Paz, D.S., Foletto, E.L., Bertuol, D.A., Jahn, S.L., Collazzo, G.C., Silva, S.S., Chiavone-Filho, O., Nascimento, C.A.O., 2013. CuO/ZnO coupled oxide films obtained by the electrodeposition technique and its photocalytic activity in phenol degradation under solar irradiation. Water Sci. Tech 68, 1031–1036.
Philippopoulos, C.J., Poulopoulos, S.G., 2003. Photo-assisted oxidation of an oily wastewater using hydrogen peroxide. J. Hazard. Mater 98, 201–210.
Polat, M., Chander, S., 2000. First order flotation kinetics models and methods for estimation of the true distribution of flotation rate constants. Int. J. Min. Process 58, 145–166.
Rattanapan, C., Sawain, A., Suksaroj, T., Suksaroj, C., 2011. Enhanced efficiency of dissolved air flotation for biodiesel wastewater treatment by acidification and coagulation processes. Desalination 280, 370–377.
Sakkas, V.A., Islam, M.A., Stalikas, C., Albanis, T.A., 2010. Photocatalytic degradation using design of experiments: a review and example of the Congo red degradation. J. Hazard. Mater. 175, 33–44.
Santander, M., Rodrigues, R.T., Rubio, J., 2011. Modified jet flotation in oil (petroleum) emulsion/water separations. Coll. Surf. A: Physicoch. Eng. Asp. 375, 237–244.
Santo, C.E., Vilar, V.J.P., Botelho, C.M.S., Bhatnagar, A., Kumar, E., Boaventura, R.A.R., 2012. Optimization of coagulation–flocculation and flotation parameters for the treatment of a petroleum refinery effluentfrom a Portuguese plant. Chem. Eng. J. 183, 117–123.
Sena, R.F., Tambosi, J.L., Genena, A.K., Moreira, R.F.P.M., Moreiraschröder, H.F., José, H.J., 2009. Treatment of meat industry wastewater using dissolved air flotation and advanced oxidation processes monitored by GC–MS and LC–MS. Chem. Eng. J. 152, 151–157.
Silva, S.S., Chiavone-Filho, O., Barros-Neto, E.L., Nascimento, C.A.O., 2012. Integration of processes induced air flotation and photo-Fenton for treatment of residual waters contaminated with xylene. J. Hazard. Mater. 199–200, 151–157.
Sun, Y., Pignatello, J.J., 1993. Photochemical reactions involved in the total mineralization of 2,4-D by $Fe^{3+}/H_2O_2$/UV. Environ. Sci. Technol. 27, 304–310.
Trinh, T.K., Kang, L.S., 2011. Response surface methodological approach to optimize the coagulation–flocculation process in drinking water treatment. Chem. Eng. Res. Des 89, 1126–1135.
Uçurum, M., 2009. Influences of Jameson flotation operation variables on the kinetics and recovery of unburned carbon. Powder Tech 191, 240–246.
USEPA-United States Environmental Protection Agency, 2000. EPA Office of Compliance Sector Notebook Project: Profile of the Oil and Gas Extraction Industry. EPA/310-R-99–006. http://www.epa.gov.
Utset, B., Garcia, J., Casado, J., Domenech, X., Peral, J., 2000. Replacement of $H_2O_2$ by $O_2$ in Fenton and photo-Fenton reactions. Chemosphere 41, 1187–1192.
Watcharasing, S., Angkathunyakul, P., Chavadej, S., 2008. Diesel oil removal from water by froth flotation under low interfacial tension and colloidal gas aphron conditions. Sep. Purif. Technol. 62, 118–127.
Yeung, C.W., Law, B.A., Milligan, T.G., Lee, K., Whyte, L.G., Greer, C.W., 2011. Analysis of bacterial diversity and metals in produced water, seawater and sediments from an offshore oil and gas production platform. Mar. Poll. Bull. 62, 2095–2105.
Yoon, R.H., 2000. The role of hydrodynamic and surface forces in bubble–particle interaction. Int. J. Min. Process 58, 129–143.
You, G., Wang, J., 2011. Laboratory study of the electrochemical pre-oxidation for improving thermodynamic stability of an oilfield produced water. J. Petrol. Sci. Eng. 76, 51–56.
Zak, S., 2009. Application of pressurized flotation process aided by hydrogen peroxide in organic sewage treatment. Ecol. Chem. Eng. 16, 42–49.